Conformation of Polymer Chain in the Bulk

J. P. Cotton,[1a] D. Decker,[1b] H. Benoit,[1b] B. Farnoux,[1a] J. Higgins,[1c] G. Jannink,[1a] R. Ober,[1d] C. Picot,[1b] and J. des Cloizeaux[1e]

Centre de Recherches sur les Macromolécules (CNRS), 67083 Strasbourg Cedex, France; Service de Physique du Solide et de Résonance Magnétique and Service de Physique Théorique, Centre d'Etudes Nucléaires de Saclay, 91190 Gif-sur-Yvette, France; Institut Max Von Laue-Paul Langevin, 38042 Grenoble, France; and Laboratoire de la Matière Condensée, Collège de France, 11, Place M. Berthelot, 75005 Paris, France. *Received May 2, 1974*

ABSTRACT: Neutron coherent scattering techniques have been used for the determination of the conformation of polymer in bulk and experimental details are given about the application of this method to the study of polymeric systems. Measurements have been made for small and intermediate momentum ranges on a series of eight monodisperse deuterated polystyrenes of molecular weight ranging from 21,000 to 1,100,000. The results lead to the concluson that in amorphous state the conformation of the polymer molecule is indistinguishable from that in θ solvent and that the Debye scattering function which is valid for unperturbed chains applies for q^{-1} as low as 10 Å.

In order to explain such properties as rubber elasticity it has long been assumed that polymer chains in the liquid state obey Gaussian statistics.[2,3] Below its glass transition temperature a polymer becomes hard and loses its elastic properties. It is believed,[4] however, that this transition affects only the motion of the drawn segments and not their configuration which is expected to remain Gaussian. There is much indirect evidence in favor of this hypothesis but until recently it has been impossible to prove it directly. Moreover, many authors[5,6] believe from theoretical considerations, electron microscopy, and diffraction results that there is more order in the amorphous state, taking the form of supramolecular structures.

In this paper, we present the results of measurements of the conformation of polystyrene molecules in the bulk amorphous state. These measurements were made using the neutron small angle scattering apparatus at the Institut Laue-Langevin in Grenoble and at the CEA Saclay. Similar experiments in this field have already been published by Kirste[7] and Ballard.[8]

The neutron SAS technique is particularly well suited to the problem for two reasons.

(1) Neutron wavelengths available from the cold sources at each of the installations are of the order of 10 Å. It is thus possible to match the experimental wave vectors to the molecular dimensions. In light scattering experiments only radii of gyration of very large molecules can be measured, while X-ray experiments need extremely small scattering angles.

(2) The difference between the neutron scattering length of deuterium and hydrogen is particularly useful since it will be shown that deuteration does not affect the thermodynamic properties of the chains and that there is perfect compatibility between deuterated and hydrogenous molecules. Thus, if deuterated molecules are embedded in a matrix of hydrogenous molecules, the scattering pattern of the former may be measured and the molecular dimensions and the statistical distribution of the chain segments deduced. The contrast is large enough for very low concentration of polymer to be used.

In the first part of the paper we give details of the neutron technique as applied to the problem of polymer conformation, then the sample preparation is described and finally the results and their interpretation are discussed.

Neutron Small Angle Scattering Technique

For experiments on polymeric systems two principal properties differentiate neutron scattering from other techniques: the interaction with the sample depends only on the neutron–nucleus interaction leading to results described in part A of this section; the wavelengths available range from 1 to 12 Å giving values of the scattering vector which are inaccessible to light and X-ray scattering. The apparatus is described in part B.

(A) Scattering Intensity. The intensity scattered by systems with long-range correlations (greater than 10 Å) takes the form of a central peak about the forward direction. The amplitude of this peak varies strongly from nucleus to nucleus. Isotopic substitution used in neutron scattering gives a powerful method of labeling molecules because it leaves the chemical properties of the molecules unchanged.

We now evaluate the scattering cross section of a mixture of labeled and unlabeled polymer molecules with a view to its application to deuterated and nondeuterated polystyrene. Using the relation for the scattered intensity which we derived, we consider the choice of sample.

(1) Scattering Cross Section. The neutron–nuclear interaction is characterized by a scattering length a_i which takes into account the spin of the isotope of the nucleus considered. The scattering cross section $\sigma(q)$per unit solid angle of a neutron of wavelength λ scattered at an angle θ by a monoatomic system consisting of N atoms at positions r_i is written[9]

$$\sigma(q) = \sum_{ij} \overline{a_i a_j} \langle e^{iq(r_i - r_j)} \rangle \qquad (1)$$

q is the scattering vector $|q| = (4\pi/\lambda) \sin \theta/2$, the bar over the scattering amplitudes denotes a spin and an isotopic averaging while the broken brackets indicate a thermal average of the function inside. $\sigma(q)$ may be written in the form

$$\sigma(q) = a^2 \sum_{ij} \langle e^{iq(r_i - r_j)} \rangle + N a_I^2 \qquad (2)$$

This relationship introduces the coherent scattering amplitude a and the incoherent scattering cross section σ_I defined by $a = \bar{a}_i$ and by

$$\sigma_I = 4\pi a_I^2 = 4\pi(\overline{a_i^2} - a^2) \qquad (3)$$

and for which tables of experimental values exist.[10,11] Thus the scattered intensity decomposes into a coherent intensity depending on the scattering vector and an incoherent intensity $N a_I^2$. Values of a and σ_I are given in Table I. It is evident from the table that the values of the scattering amplitudes of hydrogen and deuterium are very different. The transmission of the system $T = I(x)/I(0)$ is given by the equation

$$T = \exp[-d(4\pi a^2 + \sigma_I)x] \qquad (4)$$

where d is the density of the system and x the thickness of the sample.

Expression 2 takes no account of multiple scattering and can only be used when T is of the order of unity. Let us consider a system of N deuterated molecules each composed of m atoms of which the scattering amplitudes are a_α and $a_{I\alpha}$ (α varying from 1 to m). If the values of the scattering vector q are such that q^{-1} is large relative to the molecular dimensions, the structure factor of the molecule may be neglected (this is in fact always true for small scattering angles). In this case, it is possible to generalize to molecules the idea of coherent and incoherent scattering amplitudes A and A_I such that

$$A = \sum_{\alpha=1}^{m} a_\alpha \qquad A_I^2 = \sum_{\alpha=1}^{m} a_{I\alpha}^2 \tag{5}$$

and the cross section then becomes

$$\sigma(q) = A^2 S(q) + N A_I^2 \tag{6}$$

where $S(q)$ is the density fluctuation correlation function of the centers of mass R_i of the molecules

$$S(q) = \sum_{ij} \langle e^{iq(R_i - R_j)} \rangle \tag{7}$$

Using expression 5 and Table I the values of the scattering amplitudes a_H and a_{IH} of a monomer C_8H_8 of hydrogenous polystyrene and a_D and a_{ID} of a monomer of deuterated polystyrene may be calculated.

$$a_H = 2.344 \times 10^{-12}\ \text{cm} \quad a_{IH}^2 = 50.7 \times 10^{-24}\ \text{cm}^2$$
$$a_D = 10.672 \times 10^{-12}\ \text{cm} \quad a_{ID}^2 = 1.46 \times 10^{-24}\ \text{cm}^2 \tag{8}$$

Consider a system consisting of a mixture of N_A molecules of type A with cross sections A and A_I and N_B molecules of type B with cross sections B and B_I of the same volume. Using only the hypothesis of the incompressibility of the mixture we can write the scattering cross section in the form[12]

$$\sigma(q) = (A - B)^2 S(q) + N_A A_I^2 + N_B B_I^2 \tag{9}$$

which demonstrates the contrast factor $K^2 = (A - B)^2$ between the two types of molecules. $S(q)$ is the Fourier transform of the correlation function of the A molecules in the presence of B, or, which is the same thing, of holes in the ensemble B caused by the presence of A. Thus even if the coherent cross section of A is zero the scattered intensity gives the correlation between the A molecules.

(2) Signal Intensity. When the sample is a mixture of polymers of molecular weight M labeled by isotopic substitution (A) and unlabeled polymers (B) the scattered intensity may be derived from eq 9 in the form[12]

$$I(q) = \mathbf{N} V \Phi_0 t T \left[K^2 \frac{C_A}{m_A^2} M S_0(q) + \frac{C_A}{m_A} A_I^2 + \frac{C_B}{m_B} B_I^2 \right] + \int_0^t N(t,q)\, dt \tag{10}$$

where $\mathbf{N}$ is Avogadro's Number, V the volume of the system in cm^3, Φ_0 the incident neutron flux in $cm^{-2}sec^{-1}$, t the counting time in seconds, T the transmission (eq 4) of the system. C_A and C_B are the concentrations in g cm^{-3}, m_A and m_B are the molecular weights of the monomers A and B, and K^2, A_I, and B_I are the values of the contrast in scattering amplitude for the labeled and unlabeled monomers.

Table I

Atom	$a \times 10^{12}$ cm	$\sigma_I \times 10^{24}$ cm^2
H	−0.374	79.7
D	0.667	7.2
C	0.665	0.01
Ref	11	9

$S(q)$ is the Fourier transform of the correlation function between all the marked molecules, normalized to unity at $q = 0$. $N(t, q)$ is the instantaneous random noise of the apparatus. We can now discuss the amplitude of the scattered intensity and the signal to noise ratio for the two cases.

The surface area of the sample is determined by the dimensions of the incident beam and of the counter. Its thickness is such that the transmission is sufficiently high to reduce the multiple scattering. Equations 4 and 8 show that at constant transmission a sample can be ten times as thick for the deuterated matrix as for the hydrogenous matrix. However, the multiple scattering arising from an H matrix comes from the strong incoherent scattering amplitude of hydrogen and is therefore independent of scattering vector. This is not true in the case of a D matrix where the multiple scattering effects arise from the coherent scattering and are peaked in the forward direction.

The signal to noise ratio S/N, neglecting the noise of the apparatus itself, is

$$S/N = \frac{K^2 S_0(q)(M/m_A)}{A_I^2 + (C_B m_A / C_A m_B) B_I^2} \tag{11}$$

As an example we have calculated the two ratios for a solution of a polymer of molecular weight 10^5 at a concentration of 1% in the very low q region. These calculations indicate first that we have a usable S/N ratio in both situations. Table II is strongly in favor of a deuterated matrix. However, the noise of the instrument itself ($N(t, q)$) is often of the same order as the incoherent background of a PSH matrix and in practice the S/N ratio for a D matrix is only three or four times better than for an H matrix.

Moreover, any density fluctuations or impurities in the sample will produce a coherent signal which is very intense for the deuterated matrix due to its large coherent cross section and is peaked around the forward direction unlike the incoherent background from the hydrogenous matrix which is isotropic. Such a signal was observed from all fully deuterated polymer samples and proved very difficult to remove from the results. Thus in the small q range the use of a deuterated matrix is not obvious and we found an hydrogenous matrix more satisfactory. In discussing the intermediate q range we show that the same arguments hold.

(B) Apparatus. In order to study the characteristic pair correlation function of polymer samples we require scattering vectors ($q = (2\pi \sin\theta)/\lambda$) with values between 10^{-3} and 10^{-1} Å^{-1}. To reach these values the experimental arrangement must have very small scattering angles ($\theta \sim 1°$) and a long wavelength (greater than 4 Å). Furthermore in order to explore these two limits of the range of q which give precise information on chain statistics, as will be made precise in the discussion, two types of experimental arrangement are necessary and they will be described separately.

(1) General Points about the Apparatus. Continuous neutron beams come from nuclear reactors in which neutrons are produced by nuclear fission at thermal equilibrium with the moderator at a temperature of about 373°K. These neutrons are classified according to their energy E (in eV) related to the moderator temperature T (in degrees

Table II

Marked Polymer	Matrix	S/N
PSD	PSH	13
PSH	PSD	380

Table III

L, m	Vertical divergence $\times 10^3$ radians	Horizontal divergence $\times 10^3$ radians
40	13	0.8
20	2.5	1.5
10	5	3

absolute) and to the wavelength (in Å) by the equation

$$E = T/1.6 \times 10^4 = 8.18 \times 10^{-2}/\lambda^2 \quad (12)$$

The corresponding wavelength spectrum is quasimaxwellian with a maximum at about 1.8 Å. In this spectrum the intensity of wavelengths required for small angle scattering ($E < 0.005$, $\lambda > 4$ Å) is weak. The flux may be increased and the maximum of the distribution shifted to long wavelengths by locally replacing the moderator by a cold source consisting of a cell filled with liquid hydrogen or deuterium.[13,14] In this way a factor of about 10 is gained in the flux of long-wavelength neutrons ("cold neutrons").

Neutron guides[15,16] (using total internal reflection of the neutrons) remove the effective source of neutrons from the reactor itself into an adjacent experimental hall. Curved guides act also as a getter for neutrons of short wavelength. Figure 1 shows the spectrum of neutron wavelengths coming from the curved guide of the reactor EL 3 at Saclay.

Two types of monochromators were used for these experiments: either mechanical or crystalline. The first type is a helical slot velocity selector[17] with a wavelength resolution of the order of $\Delta\lambda/\lambda = 5 \times 10^{-1}$ which must be considered when interpreting the results. With a crystalline monochromator neutrons of wavelength λ are reflected according to the Bragg law. For a pyrolitic graphite monochromator the maximum wavelength is $\lambda = 6.71$ Å and the resolution $\Delta\lambda/\lambda = 10^{-2}$. For the same wavelength the intensity of monochromatic neutrons is about 50 times weaker than for a mechanical selector.

The choice between these two systems is in effect a compromise between the resolution and the signal intensity.

(2) Measurements in the Region $q < 1/R_g$. D 11 Apparatus. This apparatus[18] is constructed at the exit of a neutron guide giving a white spectrum with a maximum wavelength at 5 Å. The incident and scattered divergences may be modified by changing the distances between the source and the sample and between the sample and the detector and also the wavelength of the incident neutrons.

The apparatus is shown in Figure 2.

(a) Monochromator. Two mechanical monochromators were used in these experiments. One (A) gives a wavelength spectrum of which the width at half-height $\Delta\lambda/\langle\lambda\rangle$ is of the order of 50% (where $\langle\lambda\rangle$ is the mean wavelength of the spectrum). This half-width is constant for wavelengths between 6 and 10 Å. The second monochromator (B) has a wavelength spread $\Delta\lambda/\langle\lambda\rangle$ of 8% at a mean wavelength of 8.6 to 9 Å.

(b) Collimation. By introducing strength sections of neutron guide of 20, 10, 5, and 3 m, the distance between the effective source of neutrons (the end of the guide) and the sample may be varied between 2 and 40 m. This source

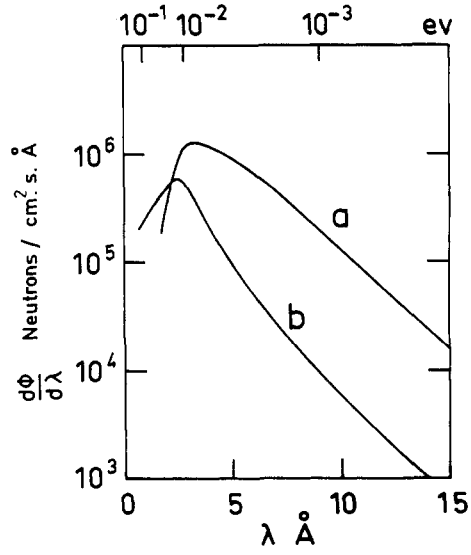

Figure 1. Plot of the logarithm of the neutron flux in Å *vs.* the wavelength λ measured at the exit of the neutron guide B I of the Saclay reactor EL 3. The curves, (a) obtained with the cold source and (b) without the cold source, show the neutron gain at large wavelength in using a cold source.

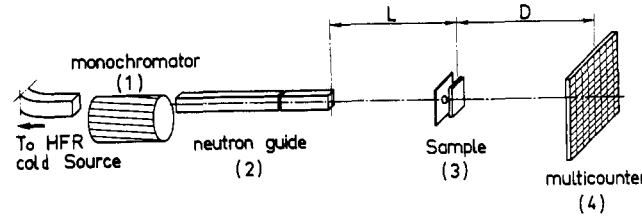

Figure 2. Scheme of the small angle apparatus D 11 of the I.L.L. high flux reactor. On the left a curved guide leads the neutron beam to the mechanical monochromator (1). Then a guide (2) of variable length translates the neutron source to a distance L from the sample (3). The scattered neutrons are registered on a multicounter (4) at variable distance D. In these experiments $L \simeq D$.

is 3 cm wide by 5 cm high. The maximum angular divergences of the incident beam for different distances L between samples and source are given in Table III.

(c) Sample Holder. The neutron beam falling on the sample is defined by a diaphragm adapted in order to match the detector cells which are of diameter 0.8 cm. For temperature-dependent measurements an automatic controlled oven was used. Measurement of sample temperature was made with an accuracy of ±0.2° and regulation was within ±0.05°. The sample cell for solutions was a metal frame with quartz windows 1 or 2 mm in thickness.

(d) Neutron Detector. The neutron detector is a BF_3 counter consisting of 64 × 64 = 4096 cells of 1 cm × 1 cm arranged in a square. Measurements were made with the multidetector at distances of 10 and 20 m from the sample (this distance is variable within ±1 m due to several different sample positions which are available).

In each experiment the neutron source was at the same distance from the sample as the detector. In these experiments, where the scattering is isotropic, cells are grouped with reference to their distance from the central cell (*i.e.*, the point where the direct beam transmitted by the sample falls). The intensity in the cells at a distance from this central cell between $R - \Delta R$ and $R + \Delta R$ is averaged and given as an intensity $I(R)$ per cm^2 ($\Delta R = 0.5$ cm), R varies from 7 to 35 cm in steps of 1 cm.

The scattering angle θ corresponding to each value of R

Table IV

Experimental setup	⟨λ⟩, Å	D, m	Monochromator	R = 7 cm θ_{min} × 10^3 rad	R = 7 cm q_{min} × 10^3 Å^{-1}	R = 35 cm θ_{max} × 10^3 rad	R = 35 cm q_{max} × 10^3 Å^{-1}
A	4	20.36	A	3.4	5.4	17.2	27
B	6.5	20.36	A	3.4	3.3	17.2	16.6
C	8.7	20.36	A	3.4	2.5	17.2	12.4
D	9.8	20.36	A	3.4	2.2	17.2	11
E	6.1	9.33	A	7.4	7.7	37.2	38.6
F	6.5	18.66	A	3.7	3.6	18.6	18
G	7.8	18.66	A	3.7	3.0	18.6	15
H	8.7	18.66	A	3.7	2.7	18.6	13
I	9.8	18.66	A	3.7	2.4	18.6	12
J	8.8	9.33	B	7.4	5.3	37.2	2.68
K	8.7	19.33	B	3.6	2.6	18	13

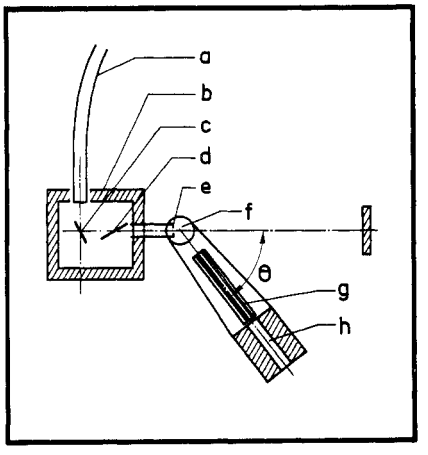

Figure 3. Scheme of the setup at the end of the curved guide B I of the Saclay reactor EL 3. One can see the cold neutron curved guide (a), the biological shielding (b), the graphite monochromator (c), the graphite filter (d), the incident collimation slit (e), the position (f) of the sample on the axis of the spectrometer, the soller slits (g) for the scattered neutron analysis, and the detector (h) in its shielding at a scattering angle θ.

is given by $\theta = R/D$ where D is the sample detector distance.

(e) Definition of Parameters and Calculation of Results. (i) Values of the Angles and Scattering Vectors. For determination of the radius of gyration R_g measurements must be made in the region $q < 1/R_g$. In Table IV we give the configuration of the apparatus and the mean wavelength ⟨λ⟩ used for these experiments. Also given are the maximum θ_{max} and minimum θ_{min} values of the scattering angle.

We were unable to perform experiments with the multidetector at 40 m from the sample because of the effect of gravity on the trajectory of the neutrons especially at long wavelengths making corrections for the wavelength spread in the beam impossible.

(ii) Wavelength Corrections. In the Guinier approximation[19] the scattered intensity is written as a function of wavelengths and of the incident neutrons intensity

$$I(q) = I(\theta,\lambda) = KI_0(\lambda)[1 - (2\pi\theta/\lambda)^2(R_g^2/3)] \quad (13)$$

where q has been replaced by $2\pi\theta/\lambda$. When the radiation is not monochromatic the measured intensity is the integrated intensity for all wavelengths. If $i(\lambda)$ is the intensity of the incident beam as a function of wavelength

$$I_0 = \int i(\lambda)d\lambda \quad (14)$$

and

$$\langle\lambda\rangle = \frac{1}{I_0}\int \lambda i(\lambda)d\lambda \quad (15)$$

$$I(\theta) = K\int[1 - (2\pi\theta/\lambda)^2R_g^2/3]i(\lambda)d\lambda \quad (16)$$

$$I(\theta) = KI_0\left[1 - (2\pi\theta)^2(R_g^2/3)(1/I_0)\int \frac{i(\lambda)d\lambda}{\lambda^2}\right] \quad (17)$$

we define $1/\lambda_0^2 = \int\lambda^{-2}i(\lambda)d\lambda/I_0$ as the mean value of λ^{-2} of the incident beam and $q_0 = 2\pi\theta/\lambda_0$. The scattered intensity in the direction θ is then written in the form

$$I(\theta) = I(q_0) = KI_0(1 - (q_0^2R_g^2/3)) \quad (18)$$

For the wavelength spread given by the two monochromators used in our experiment, we obtained

monochromator (A) $\lambda_0 = 0.95\langle\lambda\rangle$

monochromator (B) $\lambda_0 = 0.99\langle\lambda\rangle$

(3) Measurements in the Region $q \gg 1/R_g$. For values of the scattering vector $q \gg 1/R_g$ measurements are made on a two-axis spectrometer at EL 3 Saclay[12] (Figure 3). The principle of this apparatus is to define the divergence of the scattered beam by a system of antidivergent slits without changing the counter–sample distance and to use monochromatic incident neutrons, thus avoiding wavelength corrections.

(a) Monochromator. This is a monocrystal of pyrolitic graphite at the exit of a cold neutron guide. It produces a neutron beam of wavelength $\lambda = 4.62 \pm 0.07$ Å. A second graphite monocrystal eliminates the higher order contamination. The angular divergence of the incident beam is 30 min.

(b) Sample Holder. This and the oven are analogous to those described above for the D 11 apparatus.

(c) Antidivergent slits. These slits, placed between the sample and the counter, are arranged to define the scattered beam falling on the counter. The beam defined by these slits has a horizontal divergence of 30 min. The scattered wave vector, q, varies on this apparatus between 2×10^{-2} and 2×10^{-1} Å^{-1}.

Sample Preparation

The preparation of the deuterated polystyrenes was carried out under high vacuum by anionic polymerization. The absence of termination reactions during the polymerization, together with a judicious choice of the initiator and of the polymerization solvent, leads always to atactic polymers exhibiting a known molecular weight and characterized by a narrow distribution of molecular weights and absence of branching.[20]

Table V

Sample no.	PSD M_w	PSD M_w/M_n	PSD M_z/M_w	Polymerization solvent	PSH M_w	PSH M_w/M_n
1	21,000	1.05	1.05	Toluene	20,000	1.50
2	57,000	1.17	1.14	Toluene	55,000	1.08
3	90,000	1.20	1.17	Toluene	83,000	1.07
4	112,000	1.35	1.23	Toluene	114,000	1.024
5	160,000	1.13	1.13	Benzene	172,000	1.02
6	325,000	1.80	1.40	Benzene	320,000	1.04
7	500,000	1.14	1.18	Benzene	530,000	1.10
8	1,100,000	1.17	1.18	Benzene	1,170,000	1.2

Use of a nonpolar solvent and of secondary butyllithium (BuLi) as the initiator are of special interest for the polymerization of styrene.[21] In this case, the initiation and the propagation steps may be separated by an adequate change of the temperature (at t below 5°, merely initiation takes place, while propagation becomes effective above 20°). This procedure provides an easy way for removing the remaining protonic impurities from the monomer before polymerization and thus offers the best available conditions for obtaining monodisperse polymers. Before each experiment, all glass walls of the apparatus and the polymerization solvent are carefully washed with a diluted BuLi solution.

Pure secondary BuLi is obtained by distillation under high vacuum at 80° of the compound itself after having distilled off the solvent. Dilution at the desired concentration is subsequently achieved in the solvent chosen for the polymerization.

Styrene, about 99% deuterated, was provided by the CEA. The monomer is first distilled on Na wire on an apparatus fitted with a small Vigreux column, then it is distilled twice under high vacuum, on Na wire and on molecular sieves. In this way, a reasonable degree of puriirity (about 2×10^{-4} M/l. residual protonic impurities) can be reached without wasting a large amount of the expensive monomer.

The solvent chosen for the polymerization in most experiments is benzene. Toluene, which was first used, gives rise to transfer reactions with the polystyrylcarbanions[22] (transfer constant = 5×10^{-6} at 50°) so that the molecular weights of the products obtained are lower than those predicted from the ratio of the initial amounts of monomer and initiator, and the molecular weight distribution is enlarged. As expected, this side reaction exhibits an increasing influence on molecular weight and polydispersity as the monomer dilution (solvent concentration) and as the polystyrene molecular weight (ratio styrene–initiator) become higher.

The weight-average molecular weights of the samples of deuterated PS were determined by light scattering measurements in benzene or THF on a Fica apparatus. The refractive index increments, measured on a Brice-Phoenix differential refractometer, respectively 0.091 and 0.174 cm^3 g^{-1}, are noticeably lower than the corresponding increments of hydrogenated PS (0.106 and 0.198).

The polydispersity of the products was characterized by gel permeation chromatography, with use of a Water Associates apparatus combined with an automatic viscometer, THF being the solvent. The usual way of calculating the different average molecular weights (M_n, M_w, M_z) from the GPC diagrams using the log M *vs.* elution volume calibration does not fit satisfactorily, since calibration curves are different for ordinary and perdeuterated polystyrene.

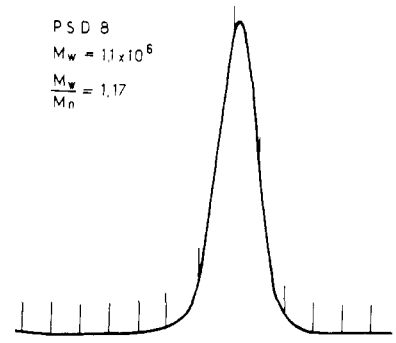

Figure 4. Gel permeation chromatography. Elution curve of sample PSD 8.

Therefore we used the so-called "universal" calibration which assumes that $[\eta]M$, measure of the particle size, is independent of the nature of the polymer.[23] From the plots of log $[\eta]M$ *vs.* elution volume, we were able to calculate back the average molecular weights. Figure 4 shows a typical elution curve. The molecular weight and polydispersity are collected in Table V. Molecular weights range from 21,000 to 1,100,000. The M_z value has been calculated, since we shall need it for correcting radii of gyration. This calculation has not taken into account the axial dispersion of the columns. It therefore gives an excess value of the polydispersity. In the last column of this table, we give the characterization of some hydrogenated polystyrene (PSH) samples which were used as matrices in some experiments.

The section of the beam in both apparatuses is of the order of 2 cm^2 and determined the surface of the sample. Its thickness 0.8 mm for a PSH matrix and 5 mm for a PSD matric has been calculated in order to have a transmission factor larger than 0.5. To be sure that this relatively small value does not introduce multiple scattering effects we have measured some samples with 0.4 mm thickness and obtained the same result.

The solid samples are disk-shaped (2 cm in diameter) with concentrations of labeled chains ranging from 0 to 2×10^{-2} g cm^{-3}.

These samples were prepared by two methods leading to the same neutron scattering results. In the first method, samples are obtained by casting dilute chloroform solutions of PSD and PSH on a mercury surface. The evaporation of the solvent is achieved under vacuum during several days. In the second method PSD–PSH mixtures are directly molded above T_g under vacuum, using a device designed by J. P. Gabel and A. J. Kovacs. These mixtures are themselves obtained by freeze drying of PSD–PSH solutions.

Results and Discussion

Typical scattered intensities are shown in Figure 5. The upper curve corresponds to the scattering by deuterated

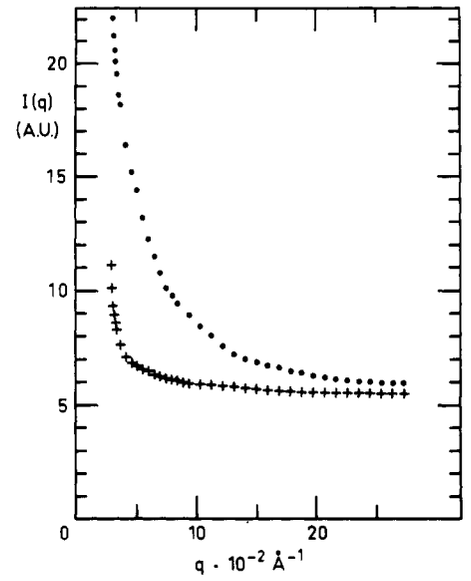

Figure 5. Experimental data obtained in the intermediate momentum range from the scattering by the PSD 1 in the H matrix and by the H matrix (+). The increase on the left of the lower curve comes from the wing of the direct beam.

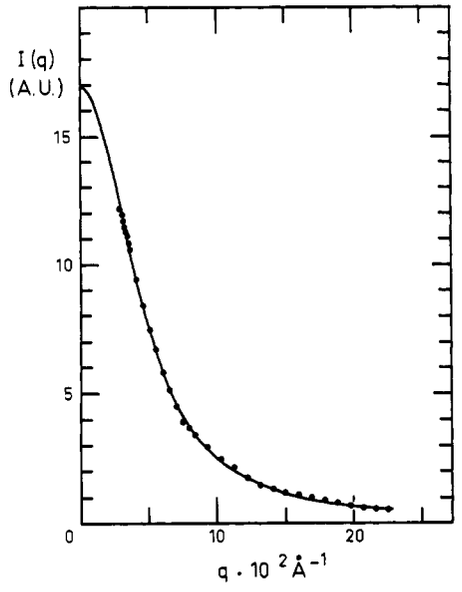

Figure 6. Intensity, in arbitrary units, obtained as a function of q by difference of the curves of Figure 5. The full line is a calculated curve which is explained at the end of this paper.

polystyrene chains of molecular weight 21,000, dispersed in a matrix of undeuterated polystyrene chains. The lower curve corresponds to the scattering by undeuterated polystyrene bulk material. Ideally this curve should show no dependence on q, at least in this range. The increase at low angle is due to the divergence of the incident beam, since even without sample such an effect is observed. The difference curve (Figure 6) is the scattering law to be interpreted. The average momentum range covered goes from 2×10^{-2} to 2×10^{-1} Å^{-1}, which includes thus a small angle scattering range $q \leq 1/R_g$ and an intermediate scattering range $q > 1/R_g$. The intensities were measured over the whole q range with the same apparatus (Figure 3). For higher molecular weights, both momentum ranges performed could not be covered with one experimental setup and thus two types of experiments were performed.

In the first, we measured the radii of gyration from the scattered intensity $I(q) = KcM(1 - (q^2R_g^2/3))$ for samples

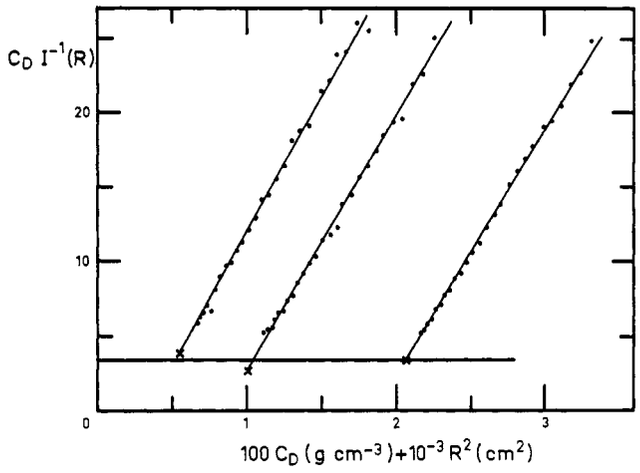

Figure 7. $C_D I^{-1}(R)$ is plotted *vs.* $C_D + R^2$ where R is a function of the scattering angle $\theta = 2\pi R/D$. The slopes of the curves give the uncorrected radius of gyration and the slope of the points (X) obtained for each C_D by extrapolation at $R = 0$ gives the value A_2 of the second virial coefficient. The data are obtained from PSD 4 in its PSH matrix.

of molecular weight M as monodisperse as possible, with eight different molecular weights, in order to test the relationship

$$\overline{R_g^2} = KM^{1+\epsilon} \tag{19}$$

where K is a constant and ϵ a parameter (it is recognized[24] that $1 + \epsilon = 2\nu$ where ν is a characteristic critical exponent) depending on the excluded volume. For this experiment, in the small momentum range, we used the apparatus in Figure 2. The results were compared with radii obtained from the same polystyrene chains and with the same technique in a good solvent (CS_2) and in a θ solvent (cyclohexane H at $T = 36°$).

The second series of measurements consisted in the analysis of the segmental configuration from the shape of the momentum dependence of the scattered intensity for larger values of q. The fact that the segments are connected in the form of a chain yields a characteristic scattering law. In the absence of excluded effect, Debye[25] has shown that

$$I(q) = KcM(2/x^2)(x - 1 + e^{-x}) \tag{20}$$

with $x = q^2R_g^2$.

When x is large and if we write $R_g^2 = b^2N/6$, b being a characteristic length associated with the statistical element, $N = M/m$ the ratio of the chain molecular weight over the statistic element molecular weight, one obtains

$$I(q) = KcM12/q^2b^2(M/m) \qquad 1/R_g < q < 1/b \tag{21}$$

These measurements were performed in the intermediate momentum range using the apparatus shown in Figure 3.

(A) Small Momentum Range. Radii of Gyration. It is known that when there are concentration effects, one has to extrapolate the radii of gyration obtained at finite concentration of labeled polymers C_D to zero C. This has been done using the Zimm procedure for a few samples in cyclohexane and in the bulk. For small concentrations, C_D of deuterated chains, and for small values of q the inverse

Table VI

PSD	M_w	R_w, Å: CS_2	Bulk	C_6H_{12} (36°)	C_6H_{12} (35°)
1	21,000	50 (E)	38 (E)	42 (A)	
2	57,000	84 (E)	59 (J)	70 (B)	
3	90,000	115 (G)	78 (F)	88 (B)	
4	112,000		87 (F)		
5	160,000	168 (G)	107 (G, K)	117 (B)	108
6	325,000	204 (G)	143 (C,F,H)	150 (B,C)	
7	500,000		213 (H,I,K)	191 (C)	
8	1,100,000	568 (I)	297 (1,K)	293 (D)	303
Technique		NS[a]	NS[a]	NS[a]	LS[b]

[a] NS = neutron scattering. [b] LS = light scattering.

scattering intensity can be represented by the Zimm formula

$$C_D KI^{-1}(\theta) = \frac{1}{M}(1 + q^2R_g^2/3) + 2A_2C_D \quad (22)$$

and the value of R_g^2 is obtained by extrapolation to $C_D = 0$. Figure 7, for instance, shows the Zimm plot which corresponds to PSD 3. Similar diagrams have been obtained on samples 1, 4, 6, and 7. Within the experimental errors no concentration effect can be detected. This result allows a simplification of the experimental procedure. In effect all the other samples were measured at only one concentration $C_0 = 10^{-2}$ g cm^{-3}, in the cyclohexane H solutions at 36° and in the bulk. Only in CS_2 have we extrapolated to zero concentration after measurements at four concentrations.

It is well known that scattering experiments do not give a weight average for the radii of gyration. More precisely if we assume between R_g^2 and M the relation of the type in eq 19, the experimental radii of gyration correspond to an average molecular weight given by the relation

$$\langle M \rangle = \left[\frac{\sum c_i M_i^{2+\epsilon}}{\sum c_i M_i}\right]^{1/(1+\epsilon)} \quad (23)$$

This average is a "z" average only if $\epsilon = 0$. Since we can expect ϵ to be small as a first approximation, which will be justified later, we replace $\langle M \rangle$ by M_z. Unfortunately, the precision of M_z is much lower than that of M_w. We therefore prefer to plot our results as functions of M_w, correcting the radii of gyration by the factor $(M_z/M_w)^{1/2}$. This factor being in most of the cases rather small, both methods are equivalent. The values obtained, which we have called R_w, are reported in Table VI. The capital letters in brackets correspond to the experimental setup (see Table IV).

In Figure 8 we have plotted log R as a function of log M_w for the three cases: deuterated polystyrene in a matrix of hydrogenated polystyrene, polystyrene in cyclohexane at 36°, and polystyrene in carbon disulfide at room temperature.

The first striking result is that in bulk the dimensions of the molecules are nearly the same as in cyclohexane (C_6H_{12} at 36°) in the entire range of molecular weights. This strongly supports the hypothesis that the sizes of the chains are identical in both situations. Since cyclohexane is at 36° a θ solvent for polystyrene, the coefficient in eq 19 is zero and R_g^2 should obey the relation

$$\overline{R_g^2} = KM \quad (24)$$

and actually in Figure 8 we have drawn a straight line of

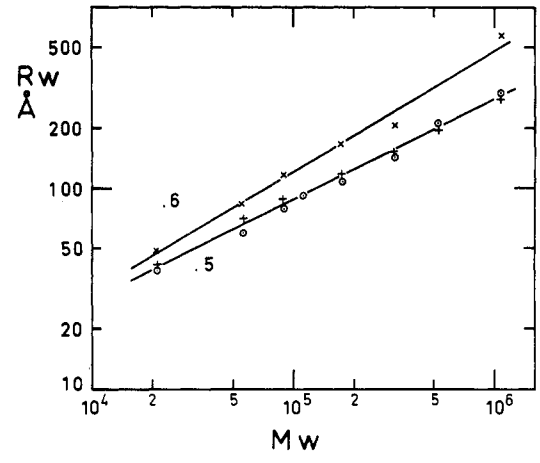

Figure 8. Log R_w is plotted *vs.* log M_w. The experimental data are obtained in different environments: (X) in a good solvent CS_2, (+) in a θ solvent, (⊙) in the bulk. The slopes of 0.6 (in CS_2) and of 0.5 are obtained by a best fit method.

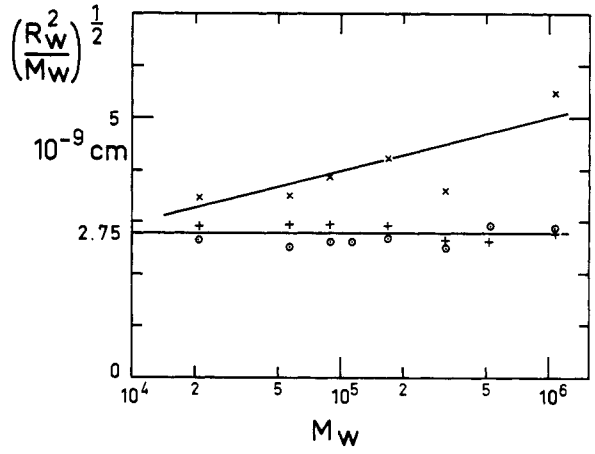

Figure 9. $(R_w^2/M_w)^{1/2}$ is plotted as a function of log M_w. The data are (X) for PSD in CS_2, (+) in θ solvent, and (⊙) in the bulk. The horizontal line, which is the mean for the data obtained in θ solvent and in the bulk, is consistent with a Gaussian configuration.

slope 0.5 which goes through the experimental points. Figure 9 shows $(R_w^2/M_w)^{1/2}$ as a function of log M_w. The horizontal straight line gives the value of $(K)^{1/2} = 2.75 \times 10^{-9}$ cm.

We note that the best fit for the cyclohexane points would not give a slope exactly equal to 0.5, but this is not surprising. For ordinary polystyrene it is well known that in cyclohexane the θ point is of the order of 35°; this could be slightly different for deuterated polystyrene. It has been shown by Strazielle, *et al.*,[26] that there is a small difference in θ temperature for deuterated polystyrene (PSD) in ordinary cyclohexane. More precisely, Strazielle has found that for PSD in C_6H_{12} the θ point is 30°, for PSH in C_6D_{12} it is 40.2°, and for PSD in C_6D_{12} it is of the order of 36°. This small difference in θ temperatures (30° instead of 36°) should be taken into account for very precise measurements. From viscosity data we can evaluate its effect as being of the order of 4% on the value of R_g. This could explain why in cyclohexane the R_g values do not vary exactly as in the bulk.

It should be noted that this comparison between values obtained in cyclohexane and in bulk is very precise, even if there is some systematic error in the absolute values, since measurements have been made in both cases with the same apparatus using the same corrections. Nevertheless, it was also important to check if the absolute values of radii of

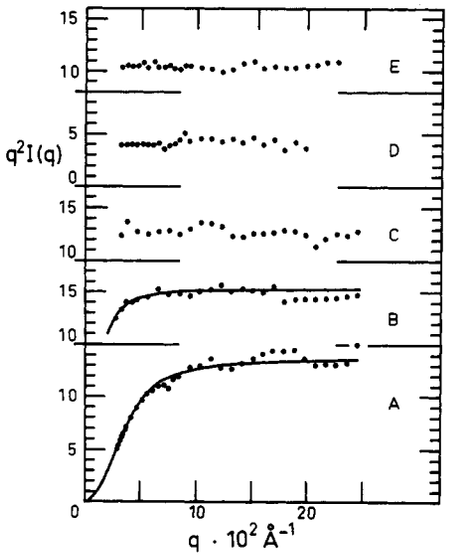

Figure 10. $q^2I(q)$ in arbitrary units is plotted *vs.* q, obtained for different samples in different environments: (A) for PSD 1 in PSH matrix, (B) for a PSH (M_w = 114,000) in a matrix of PSD 4, (C) for PSD 6 in its PSH matrix, (D) for a PSH ($M_w = 3.8 \times 10^6$) in θ solvent (C_6D_{12} 40°), and (E) for PSD 10 in its PSH matrix. The full lines are calculated curves obtained from the Debye function.

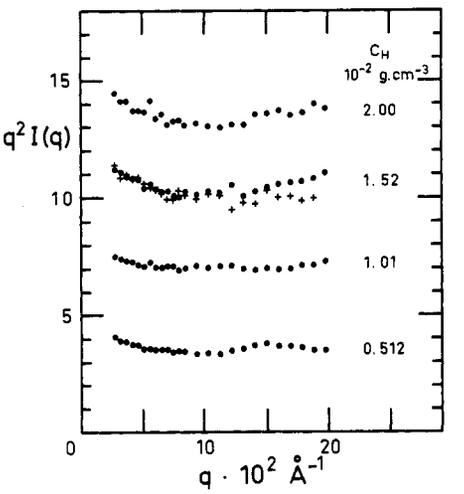

Figure 11. $q^2I(q)$ is plotted, in arbitrary units, *vs.* q. The samples are PSH ($M_w = 1.1 \times 10^6$) in a PSD 10 matrix, for the concentrations (2.00, 1.52, 1.01, and 0.512×10^{-2}g cm^{-3}). The anomalous decrease at the beginning of the curves is not an effect of multiple scattering since the sample $C_D = 1.52 \times 10^{-2}$ with a thickness of 2 mm (cross points) gives the same result as the same sample of 4 mm thickness.

gyration have been measured correctly. For this purpose we have measured the radius of gyration for two samples by light scattering. Since the principles of the measurements are exactly the same and since the same type of molecular weight average is obtained, the agreement should be good. For samples 5 and 8 in cyclohexane (30°) we measured the values of 108 and 303 Å, respectively, which are in very good agreement with the neutron results. It is well known that carbon disulfide is a good solvent for polystyrene, therefore the coefficient ϵ from eq 19 is positive and should reach its asymptotic value for large molecular weights $\epsilon \simeq 0.2$. The best straight line (Figure 8) gives

$$\overline{R_g^2} = KM^{1.2}$$

which is very satisfactory. This result demonstrates the possibilities of the neutron scattering technique for a better experimental verification of viscosity theories, since it is possible to measure simultaneously the limiting viscosity index and the dimensions of the molecules.

Effect of Temperature. It is well known that below the glass transition temperature polymeric systems are not in equilibrium. One objection to our results could be that in these experiments we are measuring frozen conformations unrelated to equilibrium properties and that the good agreement between results obtained in C_6H_{12} and in bulk is fortuitous. We would like to recall that we used two preparative techniques. In the second one where the disks are obtained by molding, all the samples have been annealed for a few hours, above T_g at 120°. No differences have been detected between the results obtained for the two types of sample.

To prove more directly that the dimensions we are measuring correspond to equilibrium conformation we have made measurements on one of our samples, 6, at 120°, having waited 36 hr to be sure equilibrium had been reached.

At room temperature we obtained 143 Å for R_g and at high temperature 134 Å. This small difference, 8%, could be due to experimental error. It could also be explained by the thermal effect on the statistical unit or unperturbed dimensions. If it is confirmed that in the bulk state volume effects can be neglected, this kind of experiment should allow study of thermal variation of unperturbed dimensions over a wide range of temperature.

Interaction between Chains. For molecular weights of samples 1, 4, 6, and 7, the intensities corresponding to four finite concentrations were measured, showing that the coefficient A_2 in eq 22 is always lower than 5×10^{-5} cm^3 g^{-2}. This raises the problem of the absence of any visible coil interaction. Since there is no chemical difference between the deuterated and the undeuterated chains, the pair correlation $g(r)$ between two deuterated segments separated by a distance r should be written as

$$g(r) = \nu_D[p(r) + (1 - p(r))\nu_D] \qquad (25)$$

where ν_D is the fraction of deuterated *vs.* total number of segments and $p(r)$ the pair correlation along a chain. The only hypothesis in this formulation is the uniform distribution of labeled segments in the matrix. The scattering intensity is proportional to the Fourier transform of $g(r)$ and this leads to

$$I(q) = MK^2S(q)\frac{C_D}{\rho}(1 - (C_D/\rho)) \qquad (26)$$

where ρ is the density of polystyrene segments, $C_D/\rho = \nu_D$, and $S(q)$ is the scattering law associated with a single chain. Formula 26 has the expected symmetry in substitution of C_D/ρ for $(1 - C_D/\rho)$. There is no scattered intensity in the limits $C_D = 0$ and $C_D = \rho$. In the limit $q = 0$, the inverse scattered intensity is then

$$C_DK^2I^{-1}(q) = (1/M) + (C_D/M) \qquad (27)$$

Comparing with eq 22, we find a second virial coefficient

$$A_2 = 1/\rho M \qquad (28)$$

This value of A_2 is always smaller than 5×10^{-5} cm^3 g^{-2} for the molecular masses used in our experiments and therefore eq 28 is not incompatible with the small experimental values of A_2.

In this discussion we have shown that the radius of gyration in the bulk is equal to the radius of gyration in cyclohexane for the same molecular weight and that $A_2 \simeq 0$. This strongly supports the hypothesis of the Gaussian character of the polystyrene chains in the bulk. Neverthe-

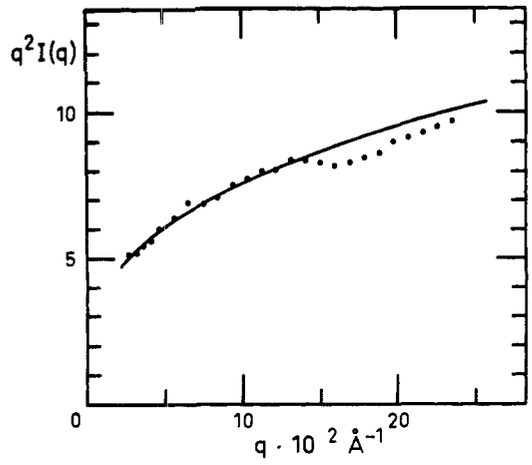

Figure 12. $q^2I(q)$, in arbitrary units, is plotted *vs.* q. The sample is PSD 10 in CS_2. The increase of this curve with increasing q is consistent with the predictions for a good solvent. The calculated curve is obtained using $n = 1.68$ in eq 29.

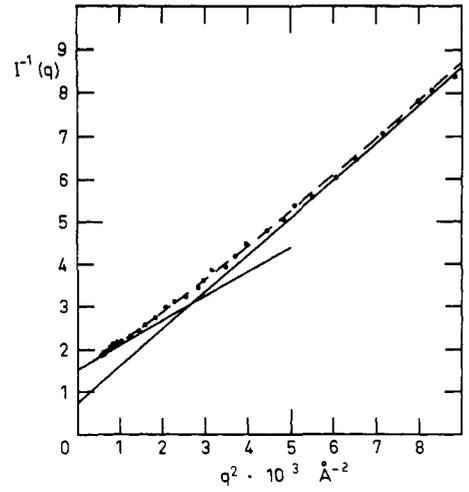

Figure 13. The curve $I^{-1}(q)$ is plotted *vs.* q for the sample PSD 1 in the H matrix. For this run the dashed line is the calculated curve for the Debye formula using a radius of gyration of 34 Å. The straight lines are the asymptotic limits of this function.

less, it could be possible, with some imagination, to find models with more or less extended and folded conformation giving the same radius of gyration. It was therefore of interest to study the intermediate range in order to see if it also confirms the preceding results.

(B) Intermediate Range. In this range $I(q)$ can be written as

$$I(q) \sim K/q^n \tag{29}$$

the exponent n being characteristic of the type of structure. If the sample is homogeneous, this value is given by $n = 1/\nu$ (the same index ν as in the definition of eq 19). For $\nu = 1$, $n = 1$, the structure is linear and the scattering objects are more or less rigid filaments. The case $\nu = \frac{1}{2}$ and $n = 2$ may correspond to random gaussian coils. However,[2] if the system is not homogeneous the case $n = 2$ may correspond to the existence of platelets of thickness small compared to q^{-1} and the case $n = 4$ to the two-density model, *i.e.*, bulky heterogeneities.

Since all previous results support the model of the random chain in the bulk state, we have tried to verify it by plotting $I(q)q^2$ as a function of q. (Some experiments carried out have shown the determinant influence of wavelength distribution on $I(q)$ behavior in the intermediate range. For this reason, measurements in this range have been made by using the monochromatic incident neutron beam of EL 3.) This is shown in Figure 10 for five samples of different types: PSD in a PSH matrix, PSH in a PSD matrix, PSH in deuterated cyclohexane at 40°. On this graph, q^{-1} varies from 30 to 5 Å. For the lower values the molecular structure of the monomers or of small groups of monomers appears already. This approach should only be used for values q^{-1} larger than 10 Å where unfortunately the signal to noise ratio is lower.

Taking these limitations into account it may be seen that $q^2I(q)$ is constant for high molecular weight, giving another confirmation of the gaussian nature of the coil. (The hypothesis of a platelet structure seems to be irrelevant and does not need to be discussed.)

The Debye formula shows that the lower the molecular weight the larger are the q values necessary to reach the asymptotic behavior. The lower curve (A) obtained for a PSD 1 (M_w = 21,000) shows that even in this case the Gaussian character is evident. The full line expresses the Debye curve obtained by a best fit method when a monodisperse system is assumed. The fit gives a radius of gyration of 35 Å. This calculated curve is also shown in the Figure 6. The value obtained by extrapolation to zero angle is 38 Å. The curve B obtained for a PSH (M_w = 114,000) dispersed in a PSD 3 matrix gives, after the same treatment, a radius of gyration of 78 Å which must be compared with the value of 87 Å (Table VI) of the PSD 4 in a PSH matrix.

In Figure 11 we have plotted, at different concentrations, $q^2I(q)$ as function of q for a high molecular weight PSH in a deuterated matrix. Even if the constancy of the product $q^2I(q)$ seems to be established there is a systematic increase of $I(q)q^2$ when q decreases. This, as we have already discussed, is probably due to structural imperfections existing in the deuterated matrix. Similar imperfections could not be observed in PSH matrices because of the much smaller coherent cross section of hydrogen. The exponent has the value 2 in eq 29 only in the absence of excluded volume effects. It is known[27] that for positive excluded volume ($\epsilon > 0$ in eq 19) n is smaller than 2; it was therefore interesting to verify if in the case of PSD solutions in CS_2 a deviation from $n = 2$ could be detected. The results are shown in Figure 12 where $q^2I(q)$ is plotted as a function of q for the concentration 2.5×10^{-3}g cm^{-3} of PSD 10. The comparison of this figure with Figures 10 and 11 shows definitively the difference between bulk and solution in a good solvent.

Conclusion

In this paper we have presented the results of a careful examination of neutron scattering from polymer chains in bulk; we have arrived at the following conclusions: (1) macromolecular chains (in bulk) have the same dimensions as in a θ solvent; (2) they obey the Debye Formula for q^{-1} as low as 5 Å. In order to show this clearly in Figure 13, we show the theoretical Debye curve and an experimental result for PSD 1 (M_w = 21,000) in an hydrogenous matrix. The fit is remarkably good and leaves very little room for other interpretation. Such a result has never been obtained by light scattering for two reasons: (a) the range of q available using this technique is very limited and it is practically impossible to have simultaneously experimental points on the initial part of the curve and on its asymptote, even with the highest available molecular weights; (b) since molecular weights must be as high as possible, samples are never monodisperse and thus produce either a straight line or downward curve instead of the expected upward curve.

This result might seem to be in contradiction to the observations on glassy polymers which have shown what has been called supramolecular structures, *i.e.*, the existence of

domains of different densities. This conflict does not in fact occur; these domains can exist as long as they do not interfere with the statistical properties of each molecular chain.

All the models of polymeric systems now proposed must take these facts into account.

Acknowledgments. This work was made possible by the CNRS who gave financial aid in the form of an ATP and by the allocation of beam time on the D 11 apparatus at the Institute Laue-Langevin (Grenoble, France). We are grateful to Dr. K. Ibel of this Institute for discussions about the use of the apparatus and to M. Rebesco and Mr. Barthelemy for assistance in running it. We would like to thank Dr. D. Cribier (CEA-SRM) for his constant help and fruitful discussions during the experiments. We also appreciate the help of Mr. M. Herbert (CEA Département des Radioéléments) in obtaining deuterated monomers.

References and Notes

(1) (a) Service de Physique du Solide et de Résonance Magnétique; (b) Centre de Recherches sur les Macromolécules; (c) Institut Max Von Laue-Paul Langevin; (d) Laboratoire de la Matière Condensée; (e) Service de Physique Théorique.
(2) (a) W. Kuhn, *Kolloid-Z.*, **68**, 2 (1934); **76**, 258 (1936); (b) H. M. James, *J. Chem. Phys.*, **15**, 651 (1947); H. M. James and E. Guth, **11**, 455 (1943); **15**, 669 (1947).
(3) P. J. Flory and J. Rehner, *J. Chem. Phys.*, **11**, 512 (1943).
(4) J. D. Ferry, "Viscoelastic Properties of Polymers," Wiley, New York, N. Y., 1970.
(5) W. Pechold, *Kolloid-Z. Z. Polym.*, **228**, 1 (1968).
(6) G. S. Yeh, *J. Macromol. Sci., Phys.* **6**, 451 (1972).
(7) R. G. Kirste, W. A. Kruse and J. Schelten, *Makromol. Chem.*, **162**, 299 (1973); *Polymer*, to be submitted for publication.
(8) D. G. Ballard, J. Schelten, and G. D. Wignall, *Eur. Polym. J.*, **9**, 965 (1973).
(9) V. F. Turchin, "Slow Neutrons," Israel Progress in Scientific Transactions Ltd., 1965.
(10) I. I. Gurevitch and L. V. Tarasov, "Low Energy Neutron Physics," North-Holland Publishing Co., Amsterdam, 1968.
(11) Tables of MIT, 1972, collected by G. Sholl.
(12) J. P. Cotton, Ph.D., University Paris VI, 1973; *CEA*, No. 1763.
(13) P. Ageron, J. M. Astruc, H. Geipel, J. Verdier, *CEA (France) BIST*, **166**, 17 (1972).
(14) D. Cribier, B. Jacrot, A. Lacaze, and P. Rousseau, IAEA Vienne, 1960.
(15) B. Farnoux, B. Hennion, and J. Fagot, IAEA Vienne, 1968.
(16) P. Ageron, P. A. Blum, *CEA (France) BIST*, **166**, 35 (1972).
(17) G. Gobert, *CEA R*, 2981 (1966).
(18) G. Degenkolbe and H. B. Greiff, *Kerntechnik*, **15**, 437 (1973).
(19) A. Guinier and G. Fournet, "Small Angle Scattering," Wiley, New York, N. Y., 1955.
(20) M. Szwarc, *Makromol. Chem.*, **35**, 132 (1960).
(21) D. J. Worsfold and S. Bywater, *Can. J. Chem.*, **38**, 1891 (1960).
(22) A. L. Gatzke, *J. Polym. Sci., Part A-1*, **7**, 2281 (1969).
(23) Z. Grubisic-Gallot, M. Picot, Ph. Gramain, and H. Benoit, *J. Appl. Polym. Sci.*, **16**, 2931 (1972).
(24) J. des Cloiseaux, *J. Phys.*, **31**, 716 (1970).
(25) P. Debye, *J. Phys. Colloid Chem.*, **51**, 18 (1947).
(26) C. Strazielle, *et al.*, in preparation.
(27) C. Loucheux, G. Weill, and H. Benoit, *J. Chimie Phys.*, 540 (1958).

Sequence Length Distribution in Segmented Block Copolymers

L. H. Peebles, Jr.[1]

Office of Naval Research, Boston, Massachusetts 02210. *Received March 18, 1974*

ABSTRACT: The effect of the nonequivalent reactivity of the two functional groups in a diisocyanate on the sequence length distribution in segmented block copolymers is calculated on a kinetic basis for a number of polymerization recipes. In the two-stage recipe, excess diisocyanate monomer first reacts completely with an intermediate molecular weight prepolymer then a low molecular weight extender is added. Alteration of the definition of the hard block segment in the two-stage process demonstrates that the distribution follows the most probable form. The heterogeneity index is less than 2 because of the relatively short sequence lengths. The number average length of the hard block segment under stoichiometric conditions at 100% conversion is equal to A_1/B_1 when the isocyanate groups are equally reactive, where A_1 is the initial concentration of diisocyanate and B_1 is the initial concentration of prepolymer. When the reactivity of the first isocyanate group becomes appreciably greater than that of the second isocyanate group, the number average length of the hard block segment approaches $(A_1 - B_1)/B_1$. The sequence length distribution of the hard blocks, the amount of internal sequences, and the molecular weight of the polymer can be varied by alteration of the polymerization recipes and the method of mixing the components.

Segmented polyurethanes are usually prepared by reacting a diisocyanate (AA) with a hydroxy-terminated polyester or polyether (BB) to form a soft block segment. The initial content of diisocyanate (AA) exceeds that of the prepolymer (BB) so that there will always be an excess of unreacted diisocyanate. The resultant polymer is then extended with a low molecular weight diol or a low molecular weight diamine (CC) to form a hard block segment. During the fabrication of the final article, the hard block portions segregate from the soft block segments to form a microheterogeneous composite.[2]

The reactions involved in this process are rather complex. The urethane bonds I formed from the reaction of isocyanate with hydroxyl and the urea bonds II formed from the reaction of isocyanate with amine are somewhat reversible. If any water is present in the system, it will react with an isocyanate group to eventually form an amine plus CO_2 gas; the amine can then react further with an isocyanate group. Branching and cross-linking reactions can occur by reaction of an active hydrogen from a urethane or a urea group with an isocyanate group to form allophonate III or biuret IV groups, respectively. In the presence of catalysts, the isocyanate groups self-polymerize to uretidione V, isocyanurate VI, or a linear polymer VII of high molecular weight. Furthermore, it has been demonstrated that the reactivity of a given isocyanate group in a diisocyanate monomer may depend strongly on whether or not the other isocyanate group has reacted.[3a]

Because of these complex reactions, little attention has been paid to the kinetics of polymerization and, in particular, to the precise composition of the soft and hard block segments. The mechanical properties of segmented polyurethanes depend strongly on the micromorphology of the finished polymer which in turn depends upon the hard and soft block composition and on the processing details. A very precise study of the effects of segment length and distribution has been undertaken by Harrell,[3b] who combined monodisperse hard segments of various lengths with soft